JOURNAL OF NANO- AND ELECTRONIC PHYSICS
Vol. **11** No 2, 02006(5pp) (2019)

ЖУРНАЛ НАНО- ТА ЕЛЕКТРОННОЇ ФІЗИКИ
Том **11** № 2, 02006(5cc) (2019)

Chalcopyrite Al(Ga, Mn)As_2 and AlGa(As, P) Quaternary Semiconductor: A First-principle Study

Byung-Sub Kang*, Kie-Moon Song**

Nanotechnology Research Center, Nano science & mechanical engineering, Konkuk University, Chungju, 27478, South Korea

(Received 18 December 2018; revised manuscript received 04 April 2019; published online15 April 2019)

The electronic and magnetic properties for a diluted magnetic semiconductor of 3*d*-metal Mn-doped $AlGaAs_2$ and $AlGa(As_xP_{1-x})_2$ chalcopyrite alloys are investigated by using the first-principle calculations. The chalcopyrite $AlGaAs_2$ and AlGa(As, P) quaternary compounds have semiconductor characters with a small band-gap. For the system of Al(Ga, Mn)As_2 chalcopyrite, the ferromagnetism with high magnetic moment of Mn is originated from the exchange couplings between Mn 3*d*- and As 4*s*-, or As 3*d*-bands. The Mn moments couple to holes by an on-site exchange interaction due to the overlap of the hole wave-function with the *d*-orbitals of the local Mn electrons. The itinerant holes of Al and Ga sites couple ferromagnetically to the local Mn-moments via the exchange interaction. While the itinerant holes in As 3*d*-, or As 4*s*-bands are aligned antiferromagnetically to the local Mn moments via the exchange interactions. When the concentration of dopants is high with over a dilute concentration, a long-range ferromagnetic state among the local moments is established by the itinerant holes. This mechanism is usually denoted as hole-carrier mediated ferromagnetism. A long-range ferromagnetism among the Mn local moments is established by the high enough hole densities of partially unoccupied majority of As 3*d*- and majority of As 4*s*-bands, by the exchange interaction between dopant Mn and the localized carriers trapped in the interstitial sites. The Al(Ga, Mn)As_2 exhibits the ferromagnetic and half-metallic states. For the increasing Mn concentration (up to 6.25 % in our work), it is maintained the ferromagnetic and half-metallic characters.

Keywords: Half-metallic, Ferromagnetism, Chalcopyrite, Spin-electronics, First-principles.

DOI: 10.21272/jnep.11(2).02006 PACS numbers: 71.15.Ap, 71.55.Gs

1. INTRODUCTION

The research on GaAs-based alloys has revealed important electronic and optical properties with many advantages such as low cost devices [1-4]. The III-V compound semiconductors, such as AlP and GaP, have a wide band-gap and possess physical properties that make them potentially interesting for the development of optoelectronics [5, 6]. The AlAs and GaP are indirect-gap semiconductors, while $AlGaP_2$ [7], AlGaAs, and AlP/GaAs compounds represent the direct-gap semiconductors. The GaP is used for manufacture of low and standard brightness red, orange, and green light-emitting diodes (LEDs). The recent experiments for Mn-doped GaP show ferromagnetism above 300 K [5, 8, 9]. The AlP is unstable in air and oxidizes rapidly, while the AlGaP is stable [7]. The AlGaAs epitaxially grown on GaAs forms the heterojunctions with perfectly matched lattices, and $Al_xGa_{1-x}As$ alloys should have a direct band-gap in the Al mole fraction range up to ~ 0.45 [10].

The AlGaP ternary material is used in devices such as visible light-emitting diodes, laser diodes, heterojuction bipolar transistors, and so on [7]. The opportunities of diluted magnetic semiconductor (DMS) devices have been limited because of low solubility of magnetic ions in non-magnetic semiconductor materials. It is one of the primary challenges to create the ferromagnetic (FM) semiconductors due to the difficulty in the spin-injection into the semiconductors to form DMS at room temperature. The GaP is a semiconductor matter for spintronics applications because it is very low lattice-mismatch to Si. Therefore, the Mn-doped GaP is an attractive matter as the magnetic sensors or data storage elements to form fast non-volatile magnetic random access memories (MRAM). However, the electron spectral range of binary III-V compound is limited. To satisfy the need of detection spectral range, the image intensifier used in the ocean exploration, ocean communication and undersea imaging is manufactured by blue extension GaAlAs/GaAs [11]. Since Al constituent can adjust the spectral response range, AlGaAs offers extensive application prospect in the detection under the condition of undersea, ocean, deserts and atmosphere.

In our paper, the electronic and magnetic properties for the Mn-doped and Mn-undoped $AlGaAs_2$, and $AlGa(As_xP_{1-x})_2$ quaternary alloys had been investigated. We observed the electronic properties, showing that both electrons and holes are capable of including ferromagnetism in this material. It is noticeable that the ferromagnetism arises from two distinguishing characteristics by *magnetic polarons* (MP) and by *hole-mediated exchange-coupling*. We predicted that the $AlGaP_2$ [12], AlGaAsP, and $AlGaAs_2$ compounds have a character of chalcopyrite (CH) semiconductor with a direct band-gap of 1.237 eV, 0.755 eV, and 0.176 eV, respectively. For the variance of As (or P) concentration, the band-gap is linearly changed. For the Mn-doped $AlGaAs_2$ compounds, the FM ordering with high magnetic moment of ~ 4 μ_B/Mn could be found.

* kangbs@kku.ac.kr
** kmsong@kku.ac.kr

2. CALCULATIONS

The CH is a class of semiconductors recognized as promising materials for nonlinear optical applications, is related to the more familiar tetrahedrally-coordinated zinc-blende (ZB) materials. The physical properties of Al(Ga, Mn)As_2 and $AlGaAs_xP_{1-x}$ quaternary alloys were investigated using the full-potential linear muffin-tin orbital (FP-LMTO) method [13, 14]. The used CH structure consists of a supercell of 64 atoms included 32 empty sites (or the interstitial sites) with one or two atoms substituted by Mn. The Mn concentrations of 3.125 % and 6.25 % were considered. The FP-LMTO method is based on a self-consistent implementation of density functional theory within the local-density approximation (LDA). The real space is divided into two regions: the muffin-tin spheres, where the charge density is described by a spherical harmonic expansion and the interstitial region, where the charge is presented by a linear combination of Hankel envelope functions having negative energies (– 1.0 Ry, – 2.0 Ry, – 3.0 Ry, in our case) [15, 16]. All calculations were performed within the generalized gradient approximation (GGA) with the exchange-correlation functional of Perdew-Burke-Ernzerhof scheme [17]. The radii of muffin-tin spheres for Mn/Ga (or Al) and As were chosen to be 2.4 (or 2.22) and 1.28 a.u., respectively. The final set of energies was computed with the plane-wave cutoff energy of 634.71 eV. The LMTO basis set and charge density in each muffin-tin sphere were expanded in terms of the spherical harmonics up to $l = 6$, where l is the angular momentum defined inside each muffin-tin sphere. The LMTO basis functions in the valence energy region were chosen as 4*s* and 3*d* for Mn, and 4*s*, 4*p*, and 3*d* for Ga (or As). The basis function of Mn (or As) for the 4*s*, 4*p*, and 3*d* was generated with cut-off energy of 163.2 eV (184.96 eV), 238.0 eV (267.92 eV), and 348.16 eV (391.68 eV), respectively. The charge density had determined self-consistently by using a gamma-centered 4 × 4 × 4 grid in the Brillouin zone.

3. RESULTS AND DISCUSSION

3.1 Chalcopyrite $AlGaAs_2$ Semiconductor

We found that the CH $AlGaAs_2$ compound exhibits the semiconducting character, which has a small band-gap of 0.176 eV as compared with the CH $AlGaP_2$ [17]. The equilibrium lattice parameters for the CH structures from first-principles calculations were obtained. The calculated lattice parameters are $a = 5.8601$ Å and $c = 11.5676$ Å for CH $AlGaAs_2$; $a = 5.8478$ Å and $c = 11.5434$ Å for CH Al(Ga, Mn)As_2 and $c/a = 1.9739$ Å. We considered the atomic relaxations for the positions of the systems. The atomic geometry and positions of the structures were fully relaxed until the force between atoms was less than 1.0 mRy/Bohr. However, the distortions of near host atoms by substituting Mn dopant in the $AlGaAs_2$ bulk were neglected. Our calculated parameters for CH AlGaAsP quaternary and $AlGaAs_2$ alloys can be compared with that of the ZB structure. The experimental values are $a = 5.65$ Å and 5.66 Å for GaAs and AlAs, respectively [18]. We summarized the calculated structural properties (lattice parameter, bulk modulus) of $AlGaAs_2$ ternary and AlGaAsP quaternary and Al(Ga, Mn)As_2 alloys in the Table 1 and Fig. 1.

In the present work, we used the supercell of 64 atoms which consists of empty lattices in two unit-cells of ZB lattice. The concentration for the $AlGa(As_xP_{1-x})_2$ quaternary alloys consists of $x = 0.0$ to 1.0. For the concentrations $x = 0$, 0.5, and 1.0, the lattices show the CH structure. The AlGaAsP and $AlGaAs_2$ are more expandable than the GaAs or AlAs. The CH AlGaAsP system exhibits the semiconducting character with the band-gap of 0.755 eV. For the $AlGa(As_xP_{1-x})_2$ system ($x = 0.0 \sim 1.0$), we can see a linear increase in the lattice parameter with respect to the increasing As concentration, while the band-gap decreases linearly from 1.151 eV to 0.176 eV with direct band-gap. The lattice parameters for each CH crystalline and the band-gaps were plotted in Fig. 1.

Table 1 – Equilibrium lattice parameters (Å), bulk modulus (GPa), Energy gap (eV), and magnetic moments (μ_B/atom) for CH AlGaAsP, $AlGaAs_2$, and Al(Ga,Mn)As_2 compounds

Compounds (CH)	Lattice parameters (a, Å)	Bulk modulus (GPa)	Energy gap (eV)	Magnetic moments (μ_B)			
				Mn	Al	Ga	As
AlGaAsP	5.7597	66.2	0.755	–	–	–	–
$AlGaAs_2$	5.8601	77.2	0.176	–	–	–	–
Al(Ga,Mn)As_2							
3.125 % Mn	5.8478	56.9	0.687*	3.97	+ 0.02	0.00	– 0.04
6.25 % Mn	5.8696	47.2	0.495*	3.97	+ 0.02	0.02	– 0.07

* denotes the quasi-energy gap

Table 2 – Cohesive energies and *l*-decomposed electrons within muffin-tin spheres on each atom at 3.125 % and 6.25 % Mn

$AlGaAs_2$ System	Cohesive Energy (eV/atom)	*s* (↑/↓)	*p* (↑/↓)	*d* (↑/↓)
Ga (3.125 % Mn)	– 6.4438	0.96 (0.48/0.48)	0.82 (0.41/0.41)	9.96 (4.98/4.98)
Ga (6.25 % Mn)		0.95 (0.48/0.47)	0.81 (0.41/0.40)	9.96 (4.98/4.98)
As (3.125 % Mn)	– 6.6849	1.36 (0.68/0.68)	1.98 (0.97/1.01)	9.98 (4.99/4.99)
As (6.25 % Mn)		1.36 (0.68/0.68)	1.99 (0.96/1.03)	9.98 (4.99/4.99)
Mn (3.125 % Mn)	– 6.6561	0.37 (0.21/0.16)	0.32 (0.18/0.14)	5.04 (4.46/0.58)
Mn (6.25 % Mn)		0.37 (0.21/0.16)	0.33 (0.19/0.14)	5.03 (4.45/0.58)

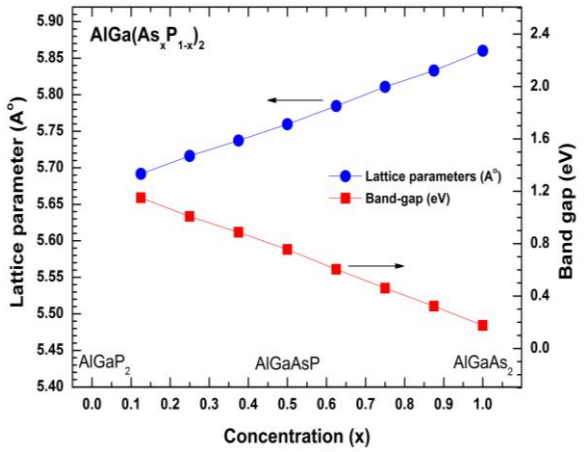

Fig.1 – Optimal lattice parameters (Å, left axis) and band-gap (eV, right axis) for CH AlGa(As$_x$P$_{1-x}$)$_2$ quaternary alloys. These values show the results with respect to the increasing As concentration

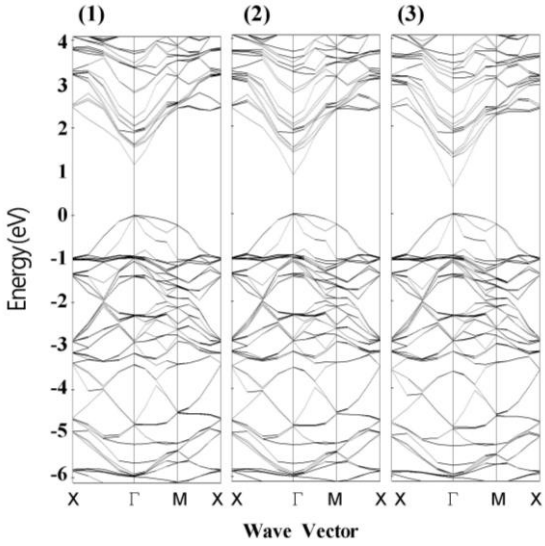

Fig.2 – Band structures for CH AlGa(As$_x$P$_{1-x}$)$_2$ quaternary alloys of (1) $x = 0.125$, (2) $x = 0.375$, and (3) $x = 0.5$. The Fermi level is set to zero

The cohesive energies for the Mn dopant, the host Ga, and the As atoms were listed in Table 2. The cohesive energy for the Mn dopant, ΔE, is determined as follows: $\Delta E = E(\text{AlGaAs}_2\text{:Mn}) - E(\text{AlGaAs}_2) - n\mu(\text{Mn})$. Here, E(AlGaAs$_2$:Mn) is the total energy of Mn-doped AlGaAs$_2$, E(AlGaAs$_2$) is the total energy of Mn-undoped AlGaAs$_2$, the integer n is the number of substituted Mn atoms, μ(Mn) is the atomic chemical-potentials of Mn for the Mn-doped CH AlGaAs$_2$ structure, the substitutional migration of Ga site by Mn dopant is more energetically favorable than that on the Al, As, or interstitial sites (empty sites). Fig. 2 shows the band structures for the CH AlGa(As$_x$P$_{1-x}$)$_2$ quaternary alloys with $x = 0.125$, 0.375, and 0.5. We can see that the CH AlGaAsP quaternary compound has a direct band-gap. The magnitudes of band-gap for $x = 125$, 0.375, and 0.5 are 1.151 eV, 0.887e V, and 0.755 eV, respectively. The band-gap is narrowed with increasing concentration of As elements. When the 3*d*-metal Mn element is doped in AlGaAs$_2$, the energy-shift occurs toward high energy. The quasi-energy gap with the 3.125 % Mn concentration exhibits an amount of 0.687 eV just above the Fermi level (E_F).

3.2 Half-metallic Ferromagnetism

Fig. 3 illustrates the density of states (DOS) for AlGaAs$_2$ and for Al(Ga, Mn)As$_2$ with 3.125 % Mn concentration. The systems of AlGaAs$_2$ and Mn-doped AlGaAs$_2$ were compared. We could observe the perturbation of the valence-band by Mn dopant in the host AlGaAs$_2$ bands. The majority-band states on the E_F are occupied by Al-3*s*, As-4*s* (or As-3*d*), and Mn-3*d* electrons mainly. This majority of d-states makes a result of strong hybridization between the As-3*d* and Mn-3d bands. The partially unoccupied Mn *e*-band (d_{x2-y2}) lies on the E_F (mainly majority-states), while the t_2-band falls into the valence-band by E_F-3.0 eV. Especially, a strong interaction between Mn-3*d* and As-3*d* occurs due to the hole-carrier accumulation between the Mn and neighboring As atoms just on the E_F. Hence the partially unoccupied *d*-bands (mainly As-3*d* and Mn-3*d* states) contribute to the ferromagnetism with high Mn magnetic moment. This configuration provides us with clues to elucidate the mechanism of *the hole-carrier mediated ferromagnetism* in Mn-doped AlGaAs$_2$. As seen from Table 1, the magnetic moments for the nearest neighboring As element from the Mn dopant is aligned negatively. The Mn-doped AlGaAs$_2$ system shows a strong *half-metallic character* due to there is no the states near the E_F in the minority-bands of host and dopant atoms. For the systems of 3.125 % and 6.25 %

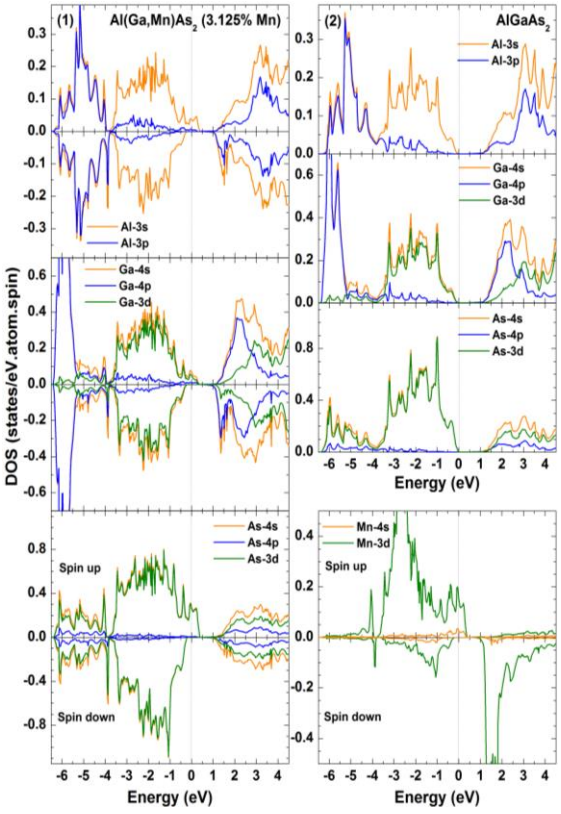

Fig. 3 – (1) DOS for Al, Ga, P, and Mn sites of Al(Ga,Mn)As$_2$ CH in the FM state, (2) DOS for Al, Ga, and As sites of CH AlGaAs$_2$. The Fermi level is set to zero

Mn-doped $AlGaAs_2$, the E_F lies in the majority-spin d states. As can be seen in Fig. 3, the partially unoccupied majority-spin *d* states are induced. This configuration of impurity *d* states may imply that the Mn-doped $AlGaAs_2$ CH system induces a high Curie temperature. As well known, the Curie temperature is strongly affected by a type in the matter and the density of carriers.

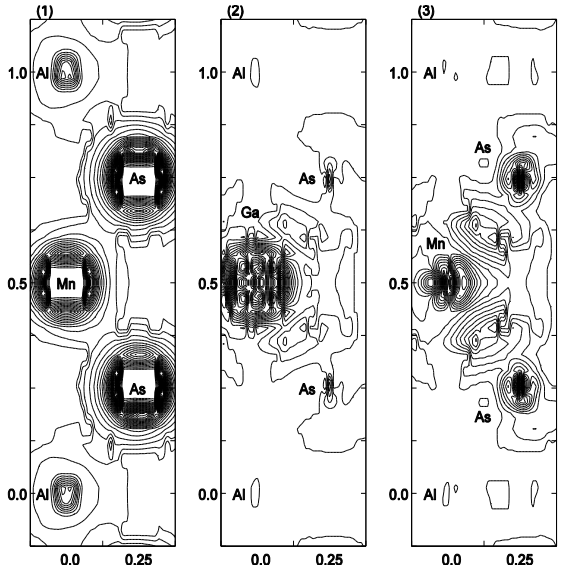

Fig. 4 – (1) Charge contour maps for CH $Al(Ga,Mn)As_2$ system, (2) and (3) the charge density difference ($\Delta\rho$) for Mn-doped $AlGaAs_2$ with the FM state. $\Delta\rho$ is defined as $\rho[Al(Ga, Mn)As_2] - \rho[Al(Ga, Mn)As_2]^M - \rho[Ga, Mn]$, where $\rho[Al(Ga, Mn)As_2]$ is the total density, $\rho[Al(Ga, Mn)As_2]^M$ and $\rho[Ga, Mn]$ are the charge densities for $Al(Ga, Mn)As_2$ with empty Mn (or Ga) site and isolated Mn (or Ga) with same lattice structure, respectively. Contour is shown on the plane (110) with intervals 7.5×10^{-4} *e*/(a.u)^3

3.3 High and Long-range FM Order

For the concentration of 6.25 % Mn in $AlGaAs_2$, the magnitude of Mn-moment shows the same values nearly with that of 3.125 % Mn. The Mn moments are coupled with holes by an on-site exchange interaction due to the overlap of the hole wave-function with the d-orbitals of the local Mn electrons. The hole density is usually heavily compensated by the antisite (antiferromagnetically aligned site) and the interstitial sites. Usually the hole density is a small fraction of 10 % order to the magnetic dopant density, since the holes become heavily compensated by the empty sites, which means that Mn is bound at a Ga and interstitial sites. For high enough hole densities, a high FM order is established through the flipping of a local Mn-moment caused by the kinetic exchange interaction with a passing-by hole. The strong kinetic exchange coupling between the holes and the Mn spins, which proves to be a high ferromagnetism in $Al(Ga, Mn)As_2$, is the basic physical mechanism underlying the occurrence of FM order. We can understand that in the disorder-free metallic systems the ferromagnetism is mediated by valence-band holes. It has been suggested that the extended hole states of the impurity-band are responsible for the establishment of the FM order. Very recent experiments have shown strong evidence that impurity-band holes play a major role, challenging the standard model for the $Ga_{1-x}Mn_xAs$ system based on the valence-band holes [19, 20].

As mentioned above, the itinerant hole couples ferromagnetically to the local Mn-moments via the exchange interaction due to the overlap of the hole wave with d-orbitals of the local Mn electrons. If the concentration of dopants is high, a long-range FM state among the local moments is established by the itinerant holes. This mechanism is usually denoted as the *hole-carrier mediated ferromagnetism*. As can be seen from the results of Table 2, for the electronic populations of each site, the electrons of dopant Mn and As atoms move to the interstitial site. The total magnetic moment in the interstitial sites is 0.133 μ_B per supercell and that of supercell shows a 3.991 μ_B. As shown in Fig. 4, it could be compared with the interaction between the Mn-Ga and Mn-As bond for the pure $AlGaAs_2$ and Mn-doped $AlGaAs_2$. We can see that a strong interaction occurs relatively by large charge accumulation between the Mn and As sites. The exchange interaction between As and Mn sites is higher than that with the other host Al or Ga sites. We can also understand that the Mn magnetic moment has mediated with the FM exchange-coupling between the neighboring Mn ions and the MP (magnetic polarons). The localized electrons trapped in the interstitial sites (empty sites) form the MP, which is stable due to the carriers are localized strongly. The FM exchange-coupling by the MP produces a long-range FM order. It is noticeable that the exchange interactions between the neighboring Mn atoms and the localized carriers trapped in the interstitial sites produce a long-range FM order.

4. CONCLUSIONS

The electronic and magnetic properties for the CH $AlGa(As_xP_{1-x})_2$ and CH $AlGaAs_2$:Mn had been investigated by using the self-consistent FP-LMTO method. The CH $AlGa(As_xP_{1-x})_2$ shows a *p*-type semiconductor character with the variance of As and P matters. The band-gap is narrowed with increasing As concentration. The Mn-doped $AlGaAs_2$ CH shows the stability of the FM state with increasing Mn concentration. The substituted system of Ga by Mn atom is the energetically favorable state. The FM ordering of Mn dopant is induced by strong coupling between Mn-3*d* and As-3*d* (or As-4*s*) orbitals mainly. A long-range FM order is maintained by high enough hole densities of the dopant and host atoms. The high magnetic moment and a long-range FM state are established by the itinerant holes which is denoted as the hole-carrier mediated exchange-coupling, and by the exchange-coupling of Mn ions by the MP. Even though the Mn concentration increases, the CH $Al(Ga, Mn)As_2$ quaternary alloys exhibit the FM and the half-metallic ground states. We had observed the quasi-energy gap by amount of ~ 0.5 eV for the CH Mn-doped $AlGaAs_2$ with the concentration of 3.125 % and 6.25 % Mn. Even though it is necessary to study more in the DMS limit, we expect it to be an application of useful DMS in the spintronics.

AKNOWLEDGEMENTS

This work was supported by Konkuk University (Dept. of Nano science and Mechanical engineering) in 2018.

REFERENCES

1. H. Ohno, A. Shen, F. Matsukura, A. Oiwa, A. End, S. Katsumoto, Y. Iye, *Appl. Phys. Lett.* **69**, 363 (1996).
2. T. Jungwirth, J. Simova, J. Mašek, J. Kučera, A.H. MacDonald, *Rev. Mod. Phys.* **78**, 809 (2006).
3. I. König, J. Schliemann, T. Jungwirth, A.H. Macdonald, *Electronic Structure and Magnetism of Complex Materials* (Ed by D.J. Singh, D.A. Papaconstantopoulos (Springer Verlag, Berlin), 163 (2003).
4. T. Dietl, *Modern Aspects of Spin Physics* (Ed by W. Pötz, J. Fabian, U. Hohenester (Springer, Berlin), 1 (2007).
5. N. Thodoropoulou, A.F. Hebard, M.E. Overberg, C.R. Abernathy, S.J. Pearton, S.N.G. Chu, R.G. Wilson, *Phys. Rev. Lett.* **89**, 107203 (2002).
6. S. Adachi, *Physical Properties of III-V Semiconductor Compound: InP, InAs, GaAs, GaP InGaAs, and InGaAsP* (Wiley: New York: 1992).
7. M.E. Overberg, G.T. Thaler, R.M. Frazier, C.R. Abernathy, S.J. Pearton, R. Rairigh, J. Kelly, N.A. Theodoropoulou, A.F. Hebard, R.G. Wilson, J.M. Zavada, *J. Vac. Sc. Technol. B* **21**, 2093 (2003).
8. T. Dietl, *J. Appl. Phys.* **89**, 7437 (2001).
9. M.E. Overberg, B.P. Gila, G.T. Thaler, et al., *J. Vac. Sci. Technol. B* **20**, 969 (2002).
10. W. Lu, R.P. Campion, C.T. Foxon, E.C. Larkins, *J. Crystal Growth* **312**, 1029 (2010).
11. F. Shi, J. Zhan, H.C. Cheng, *Spectrosc. Spectral. Anal.* **32**, 297 (2012).
12. Byung-Sub Kang, Kwang-Pyo Chae, Haeng-Ki Lee, *Adv. Condens. Matter Phys.* ID 706957, 1 (2015).
13. O.K. Andersen, *Phys. Rev. B* **12**, 3060 (1975).
14. S.Y. Savrasov, *Phys. Rev. B* **54**, 16470 (1996).
15. O.K. Andersen, O. Jepsen, *Phys. Rev. Lett.* **53**, 2571 (1984).
16. P. Kruger, M. Taguchi, S. Meza-Aguilar, *Phys. Rev. B* **61**, 15277 (2000).
17. J.P. Perdew, K. Burke, M. Ernzerhof, *Phys. Rev. Lett.* **77**, 3865 (1996).
18. C. Kittel, *Introduction to Solid State Physics,* seventh ed. (John Wiley & Sons), chap. 1 (1996).
19. Bouzerar, G.T. Ziman, J. Kudrnovoky, *Phys. Rev. B.* **72**, 125207 (2005).
20. K.S. Burch, D.B. Shrekenhamer, E.J. Sinley, J. Stephens, B.L. Sheu, R.K. Kawakami, P. Schiffer, N. Samarth, D.D. Awschalom, D.N. Basov, *Phys. Rev. Lett.* **97**, 87208 (2006).

Чотирикомпонентний напівпровідник халькопіритів Al(Ga,Mn)As$_2$ та AlGa(As,P): дослідження базових принципів

Byung-Sub Kang, Kie-Moon Song

Nanotechnology Research Center, Nano Science & Mechanical Engineering, Konkuk University, Chungju, 27478, South Korea

Досліджено електронні та магнітні властивості розбавленого магнітного напівпровідника халькопіритних сплавів AlGaAs$_2$ та AlGa(As$_x$P$_{1-x}$)$_2$ з легованим 3*d*-металом Mn, використовуючи перші принципи. Халькопіритні чотирьохкомпонентні сполуки AlGaAs$_2$ and AlGa(As, P) мають напівпровідникові характеристики і невелику заборонену зону. Для системи халькопіриту Al(Ga, Mn)As$_2$, феромагнетизм з високим магнітним моментом Mn виникає з обмінних зв'язків між Mn 3*d*- and As 4*s*-, or As 3*d*-смугами. Моменти Mn приєднуються до дірок шляхом обмінної взаємодії за рахунок перекриття хвильової функції дірки з *d*-орбіталями локальних Mn-електронів. Вихідні отвори Al і Ga-ділянок феррромагнітно з'єднуються з локальними Mn-моментами за допомогою обмінної взаємодії. У той час як прохідні отвори в As 3*d*-, або As 4*s*-смугах вирівнюються антиферомагнітно до локальних моментів Mn за допомогою обмінних взаємодій. При концентрації легуючих домішок більшою ніж розбавлена концентрація, далекодіючий феромагнітний стан між локальними моментами встановлюється мандруючими дірками. Цей механізм зазвичай позначається як ферромагнетизм, опосередкований дірками. Далекодіючий феромагнетизм серед локальних моментів Mn визначається досить високою щільністю дірок частково незайнятої більшості As 3*d*- та As 4*s* смуг, за допомогою обмінної взаємодії між легуючою домішкою Mn і локалізованими носіями, які потрапили в інтерстиціальні ділянки. Al(Ga, Mn)As$_2$ демонструє феромагнітні і напівметалеві стани. При збільшенні концентрації Mn (до 6.25 % у нашій роботі) зберігаються феромагнітні та напівметалічні характеристики.

Ключові слова: Напівметалеві характеристики, Феромагнетизм, Халькопірит, Спінова електроніка, Перші принципи.